Int. J. Electrochem. Sci., 16 **(2021)** Article ID: 210237, doi: 10.20964/2021.02.05

International Journal of
ELECTROCHEMICAL
SCIENCE
www.electrochemsci.org

A Novel Electrochemical Biosensor based on Layered Hydroxide Nanosheets/DNA Composite for the Determination of Phenformin Hydrochloride

Jing Li[1,*], *Jie Bai*[2], *Li Dong*[3], *Miao Yang*[1], *Yaping Hu*[1], *Li Gao*[1], *Huiqin Qian*[1]

[1] School of Basic Medicine, Sanquan College of Xinxiang Medical University, Xinxiang, Henan 453003, China
[2] College of Chemistry and Chemical Engineering, Xiamen University, Xiamen 361005, China
[3] School of Basic Medicine, Xinxiang Medical University, Xinxiang, Henan 453003, China
[*]E-mail: jingli_sanquan@163.com

Received: 16 June 2020 / *Accepted:* 22 November 2020 / *Published:* 31 December 2020

Layered double hydroxides (LDHs) are a kind of lamellar materials, which have been widely developed in electrochemical sensor owing to their excellent properties, such as large specific surface area, unique ion-exchange characteristic and good biocompatibility. In this paper, we reported a novel electrochemical sensor through layer-by-layer self-assembly of ultra-thin LDH nannosheets (LDHNS) and DNA for detecting the phenformin hydrochloride. The voltammetric signal of guanine in DNA/LDNHS hybrid decreases evidently due to the strong interaction between DNA and phenformin hydrochloride. Benefit from the synergic effect of LDHNS and DNA, the electrochemical sensor shows a wide linearity range from 1.0×10^{-5} mol·L^{-1} to 1.0×10^{-3} mol·L^{-1} with a low detection limit of 3.4×10^{-6} mol·L^{-1}. Furthermore, the interaction between phenformin hydrochloride and DNA on modified electrode is also studied by electrochemical method and UV-vis spectroscopy.

Keywords: Electrochemical biosensor; DNA; Layered double hydroxides; Layer-by-layer assembly; Phenformin hydrochloride

1. INTRODUCTION

Electrochemical sensors have attracted much attentions as the promising detection method for the electrochemically active biological molecules and environmental pollutants owing to the numerous advantages, such as rapid response, high sensitivity, excellent selectivity and low detection cost [1-3]. Among these sensors, DNA electrochemical sensor is a kind of sensor device with high specificity and molecular recognition that based on the electrochemical signals of the electroactive purine bases after interacting with the analyte molecules [4-9]. However, there are remains challenges for the fabrication

of DNA electrochemical sensors. On the one hand, the unstable immobilization of DNA is the primary problem due to the weak interaction between the DNA and conventional electrodes. On the other hand, the electrochemical signals of DNA bases are generally weak on conventional electrodes, which influence the sensitivity seriously. Therefore, the additional supporting materials are employed to enhance the performance of the DNA electrochemical sensors [10-11].

Layered double hydroxides (LDHs) are a kind of layered materials with two-dimensional nanostructures, which consist of positively charged layer with charge balancing anions and water molecules between the layers. The chemical composition of LDHs can be expressed as $[M^{II}_{1-x}M^{III}_{x}(OH)_2]^{x+}(A^{n-})_{x/n}\cdot yH_2O$, where M^{II} is divalent cations, M^{III} is trivalent cations, A^{n-} is interlayer anion, and x is stoichiometric coefficient. LDHs have been widely developed in the field of electroanalysis due to their large specific surface area and excellent biocompatibility [12]. However, LDHs are generally in powder form, which leads to low utilization, poor contact efficiency and difficulties in separation. Exfoliating the LDHs is an effective way to solve abovementioned problems. Inheriting the advantages of LDHs, the exfoliated LDH nanosheets (LDHNS) possess nanoscale thickness and submicron-scale to micron-scale transverse dimensions, which improve the specific surface area significantly. More importantly, the layers of LDHs display positive charges after exfoliating, which is considered a promising candidate to attract the negatively charged DNA through layer-by-layer self-assembly (LBL) method [13-15].

Phenformin hydrochloride (Fig. 1) is an antidiabetic drug once used for the treatment of adult noninsulin dependent and part of insulin-dependent diabetes mellitus, which has been banned in many countries because of its severe side effects [16]. However, the abuse of phenformin hydrochloride still exists especially in some clinics or economically underdeveloped areas. Therefore, the detection of phenformin hydrochloride is crucial for the development of health care. The methods of detecting phenformin hydrochloride mainly include ultraviolet spectrophotometry [17], HPLC [18], potentiometr titration [19], four benzene boron sodium method [20], capillary electrophoresis [21], chemiluminescence [22]. However, the above mentioned methods generally involve complex instruments, complex operation process, or toxic organic reagents.

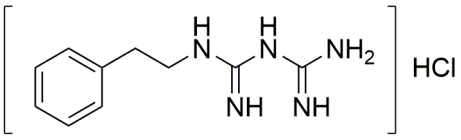

Figure 1. Structure of the phenformin hydrochloride

In this paper, we fabricate a novel DNA electrochemical sensor by integrating Ni-Al-LDHNS with DNA through LBL method for efficiently detecting phenformin hydrochloride. Because of the interaction between the phenformin hydrochloride and DNA, the electrochemical signal changes of DNA bases are recorded as the detecting characteristics. Besides, LDHNS provides a good biocompatibility microenvironment for DNA. Benefit from the synergic effect of LDHNS and DNA, the electrochemical sensor shows a wide linearity range from 1.0×10^{-5} mol·L^{-1} to 1.0×10^{-3} mol·L^{-1} with a low detection limit of 3.4×10^{-6} mol·L^{-1}. Furthermore, the interaction between phenformin hydrochloride and DNA is also studied by electrochemical method and UV-vis spectroscopy.

2. EXPERIMENTAL

2.1. Reagents and methods

PEI (50% by mass) was purchased from Aldrich. Nafion was purchased from Aldrich, which was diluted to 0.5% with ethanol solution (ethanol with water 85:15) [23] before using. Phenformin hydrochloride standard sample (99.7%) was purchased from National Institute for the Control of Pharmaceutical and Biological Products. Double-stranded herring sperm DNA (dsDNA) was obtained from Sigma. The aqueous solutions were prepared by Milli-Q system. Stock solution of DNA was prepared by dissolving 10 mg DNA in 1.0 mL Tris-HCl buffer by shaking gently and stored at 4 °C. The concentration of DNA solution was determined by UV absorbance at 260 nm using an extinction coefficient (ε_p) of 6600 $M^{-1}cm^{-1}$. Single-stranded DNA (ssDNA) was produced by heating the dsDNA solution in a water bath at 100 °C for 10 min, immediately followed by rapid cooling in an ice bath. Phosphate buffered solutions (PBS) were prepared using 0.1 $mol \cdot L^{-1}$ Na_2HPO_4 and 0.1 $mol \cdot L^{-1}$ KH_2PO_4. All other chemicals were analytical grade.

2.2. Apparatus

All the electrochemical measurements were performed in a conventional three-electrode cell controlled by CHI660D electrochemical workstation (CH Instruments, Shanghai, China). A glassy carbon electrode (GCE, 3 mm diameter) was used as working electrode, and a saturated calomel electrode (SCE) and platinum electrode were used as reference electrode and auxiliary electrode, respectively. All solutions were purged with high-purity nitrogen for at least 20 min prior to experiments. Electrochemical impedance spectra was measured with frequencies varying from 0.01 to 100, 000 Hz and amplitudes of 0.005 V in 10 $mmol \cdot L^{-1}$ $K_3[Fe(CN)_6]$/ $K_4[Fe(CN)_6]$ (1:1) in 0.1 $mol \cdot L^{-1}$ KCl. X-ray diffraction (XRD) measurements were carried out on a powder X-ray diffraction (XRD) system (X' Pert PRO MPD), equipped with Cu-Ka radiation at 40 kV, 40 mA. UV-vis spectroscopy was measured at a TU-1901 double beam UV-vis photometer (Puxi General Instruments, Beijing, China)

2.3. Synthesis of Ni-Al-LDH nanosheets

The Ni-Al-LDH nanosheets were prepared according to the reported method [24]. In a typical procedure, 0.4 $mol \cdot L^{-1}$ NaOH and 0.1 $mol \cdot L^{-1}$ Na_2CO_3 aqueous solution were mixed to 50 mL and sonicated for 30 min. Then, the mixed solution was added into 50 mL mixed salt solution of $Ni(NO_3)_2$ (0.15 $mol \cdot L^{-1}$) and $Al(NO_3)_3$ (0.05 $mol \cdot L^{-1}$) under continuous stirring at room temperature. The pH value of the solution was adjusted to 10.5 through adding NaOH solution (0.4 $mol \cdot L^{-1}$). The suspension was stored at 60 °C for 24 h, and then washed to neutral pH and dried at 80 °C for 24 hours. The product was grinded and added into a salt-acid solution containing $Ni(NO_3)_2$ (0.075 $mol \cdot L^{-1}$) and HNO_3 (0.0025 $mol \cdot L^{-1}$), adn the mixture was stirring at room temperature for 24 h. The product was centrifuged and washed with water until the pH of the washings was around 7.0. Subsequently, the

product was dried in vacuum for 12 h under 70 °C, and dispersed in formamide and stirred for 72 h under nitrogen atmosphere.

2.4. Assembly of the GCE/PEI/Nafion/LDHNS/DNA

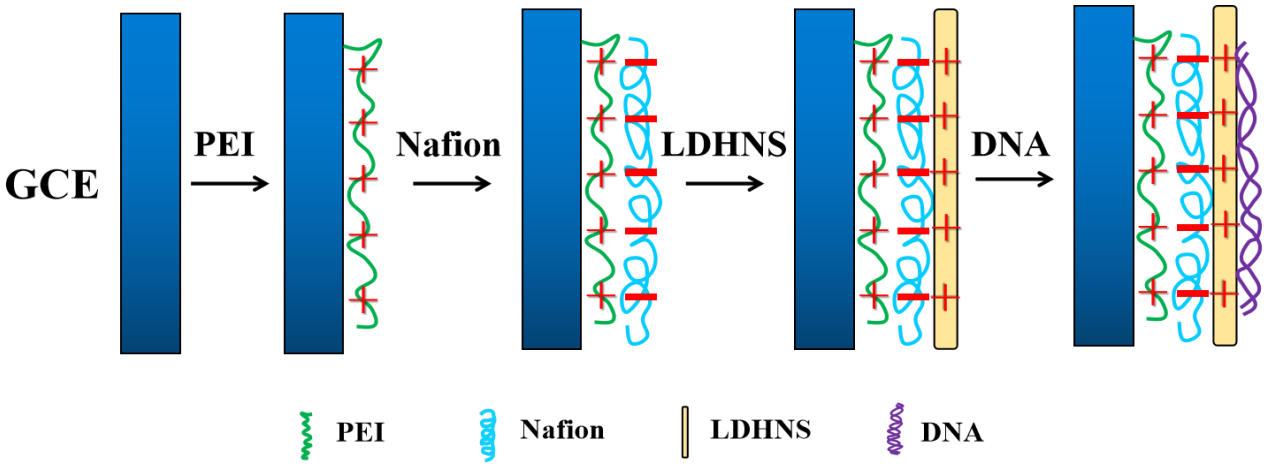

Figure 2. Schematic of the fabrication process of GCE/PEI/Nafion/LDHNS/DNA biosensor.

The biosensor was fabricated according to the following procedure, as shown in Fig. 2. GCE (3 mm in diameter) was polished with alumina and then sonicated with water and ethanol for 3 min and dried in air. The cleaned GCE was firstly dipped into the cationic PEI solution (2.5 mg·mL^{-1}) for 15 min and anionic Nafion solution (0.5%) for 20 min. Then, the modified GCE with negative charges was immersed into LDH nanosheets colloidal suspension (0.5 mg·mL^{-1}) for 30 min and 10 mg·mL^{-1} DNA (dsDNA and ssDNA) stock solution for 30 min at 4 °C, respectively. Each assembly step was followed by thorough washing and drying in air. Finally, the GCE/PEI/Nafion/LDHNS/DNA (dsDNA and ssDNA) biosensors were obtained.

3. RESULTS AND DISCUSSION

3.1 Characterization of LDH nanosheets

Fig. 3 shows the XRD patterns of the synthesized Ni-Al-LDH and exfoliated Ni-Al-LDH nanosheets. The XRD patterns of Ni-Al-LDH (curve a) exhibit the sharp hydrotalcite characteristic peaks of (003), (006), and (012) and the appearance of peak 2 θ = 10.3° (003) proves the success of ion exchange [21]. In comparison, these characteristic diffraction peaks are not found in the exfoliated Ni-Al-LDH nanosheets, indicating that the layered orderly structure is destroyed [25]. The broad diffraction peak 2 θ = 20 ~ 30° is caused by the long-range disorder of LDHs after exfoliation, which further suggests the Ni-Al-LDH was exfoliated successfully [25].

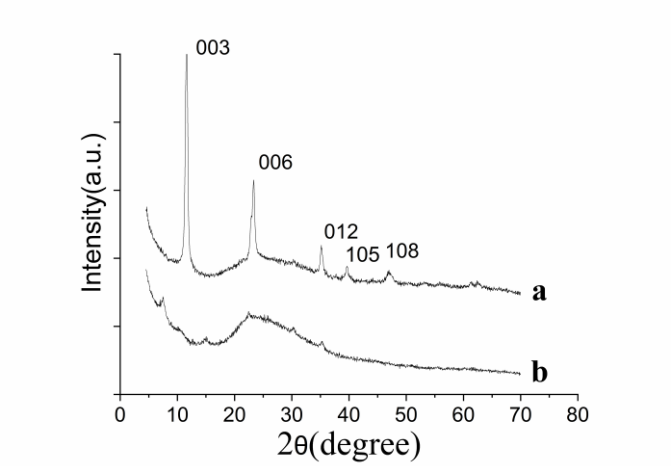

Figure 3. XRD patterns of the Ni-Al-LDH (a) the exfoliated Ni-Al-LDH nanosheets (b).

3.2 Characterizations of the assembly process of GCE/PEI/Nafion/LDHNS/DNA

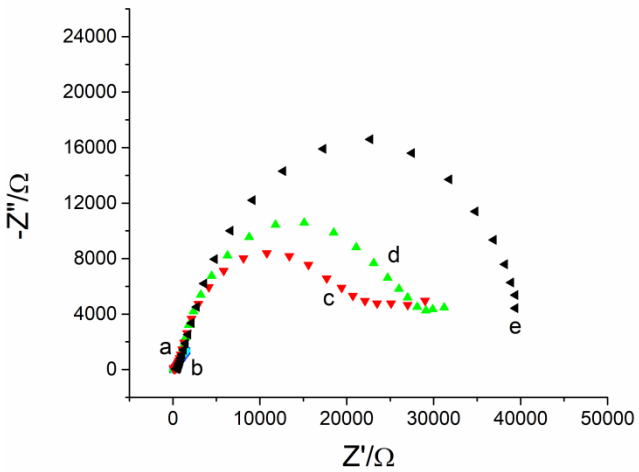

Figure 4. EIS of GCE (a), GCE/PEI (b), GCE/PEI/Nafion (c), GCE/PEI/Nafion/LDHNS (d), GCE/PEI/Nafion /LDHNS/DNA (e) in 10 mmol·L^{-1} $K_3[Fe(CN)_6]/K_4[Fe(CN)_6]$ (1:1) in 0.1 mol·L^{-1} KCl

Electrochemical impedance Spectroscop (EIS) is a useful method to study the interfacial properties of modified electrodes. Fig. 4 illustrates the Nyquist plots of various modified electrodes in 10 mmol·L^{-1} $K_3[Fe(CN)_6]/K_4[Fe(CN)_6]$ (1:1) in 0.1 mol·L^{-1} KCl. For bare GCE (curve a), the electron transfer resistance (R_p) is estimated to be 20 Ω. After the modification of PEI (curve b) and Nafion (curve c), the R_p value was varied to nearly 0 Ω and 1.4×10^4 Ω, respectively, which is ascribed to the promotion of the positively charged PEI and hindrance of the negatively charged Nafion to the electron transfer of $[Fe(CN)_6]^{3-/4-}$ [26]. When the LHDNS was assembled (curve d), the positively charged LHDNS can attracts the negatively charged $[Fe(CN)_6]^{3-/4-}$ probe through electrostatic interaction, thus leading to the decreased R_p value of 6×10^3 Ω. As the DNA was immobilized to complete the biosensor (curve e), the R_p is finally increased to 7×10^5 Ω. This is because the negatively charged DNA

macromolecule and the thick modification layer, which hinder the electron transfer [27]. The above results demonstrate that PEI, Nafion, LDHNS and DNA were successfully modified on the electrode surface through LBL method.

3.3 Electrochemical behavior of DNA immobilized on GCE/PEI/Nafion/LDHNS/DNA biosensor

3.3.1 Comparison of electrochemical responses of DNA immobilized on different electrodes

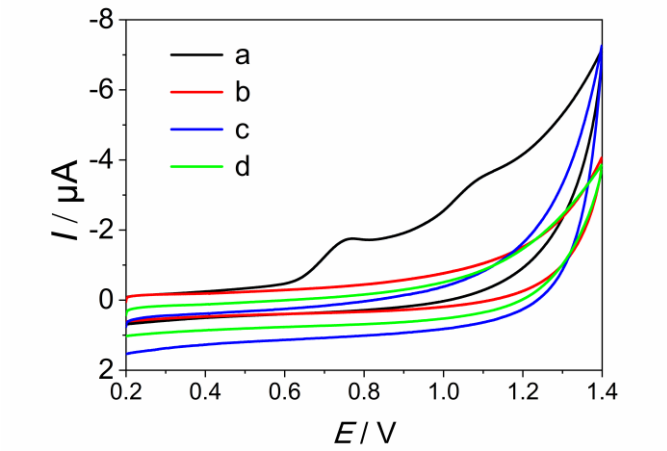

Figure 5. CV curves of several biosensors in PBS (pH 7.0) (a) GCE/PEI/Nafion/LDHNS/DNA, (b) GCE/PEI/Nafion/LDHNS, (c) GCE/DNA, (d) GCE/PEI/Nafion/DNA

All four bases of DNA (guanine, adenine, cytosine, and thymine) are electrochemically active. Among these four bases, guanine is most susceptible to oxidation, but its oxidation peak current is difficult to be observed on bare GCE [28]. Figure 5 shows the cyclic voltammetry (CV) curves of several biosensors measured in PBS. Two obvious anodic peaks at 0.668 V and 0.960 V, corresponding to the oxidation of guanine and adenine [29], were achieved in GCE/PEI/Nafion/LDHNS/DNA biosensor (curve a). In comparison, such anodic features of DNA were not observed in other biosensors, indicating the existence of LDHNS improve the electrochemical response of DNA significantly. On the one hand, the positively charged LDHNS possess large specific surface area, which promotes the adsorption of the negatively charged DNA chains. On the other hand, the LDHNS assembled through LBL method provide a favorable microenvironment for DNA, thus facilitating the electron transfer between DNA and electrode [30].

3.3.2 Influences of DNA concentration and layer number

To optimize the electrochemical signal, we further explored the DNA concentration and layer number for the fabrication of the biosensor. Figure 6A shows the influence of DNA concentration under the same immersion time (30 min) on the oxidation peak current of the guanine. When the DNA concentration changed from 5 mg·mL^{-1} to 20 mg·mL^{-1}, the peak current of guanine increased to the maximum at 10 mg·mL^{-1} and then decreased with the increased DNA concentration. Figure 6B shows

the influence of layer number on the electrochemical response of biosensor under the same assembly condition. The biosensor with monolayer DNA displays larger oxidation peak current of guanine than that with bilayer. This is possibly due to the increased electric resistance caused by the thick DNA film, which hinders the electron transfer between DNA and electrode seriously. As a result, the monolayer DNA assembled with the concentration of 10 mg·mL^{-1} is optimal for the fabrication of the biosensor.

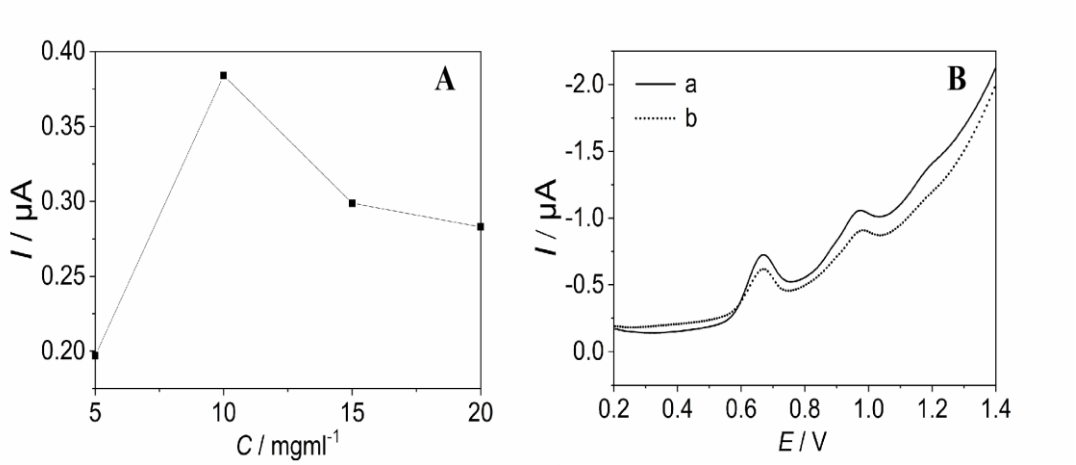

Figure 6. (A) Influences of DNA concentration on the CV peak current of guanine on GCE/PEI/Nafion/LDHNS/DNA biosensor. (B) Influences of layer number on the DPV peak current of guanine on GCE/PEI/Nafion/LDHNS/DNA, (a) GCE/PEI/Nafion/LDHNS/DNA, (b) GCE/PEI/Nafion/(LDHNS/DNA)$_2$, which represents the biosensor with DNA bilayer.

3.4 Electrochemical detection of phenformin hydrochloride on GCE/PEI/Nafion/LDHNS/DNA biosensor

3.4.1 Comparison of electrochemical responses of phenformin hydrochloride on different electrochemical sensors

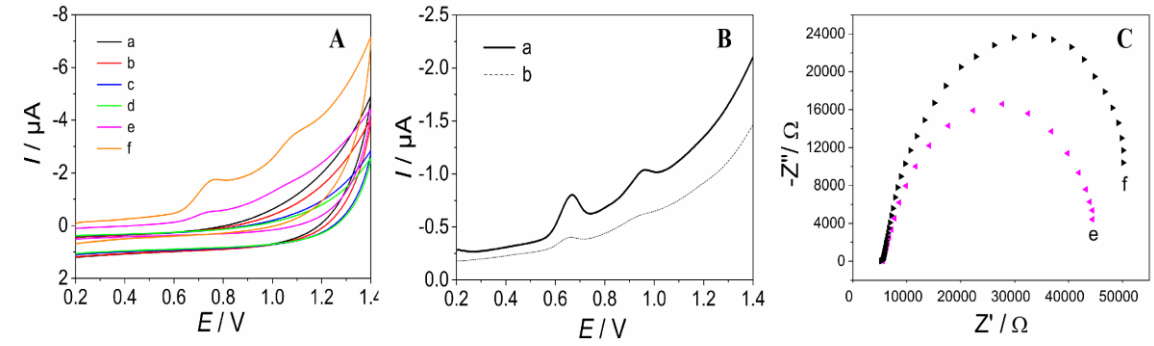

Figure 7. (A) CV curves of GCE (a, b) and GCE/PEI/Nafion/LDHNS modified electrode (c, d), and GCE/PEI/Nafion/LDHNS/DNA modified electrode (e, f) in PBS (pH 7.0) without (a, c, f) and with (b, d, e) 1.0×10^{-3} mol·L^{-1} phenformin hydrochloride. (B) DPVs of GCE/PEI/Nafion/LDHNS/DNA in PBS (pH 7.0) without (a) and with (b) 1.0×10^{-3} mol·L^{-1} phenformin hydrochloride. Scan rate: 100 mV·s^{-1}. (C) EIS of GCE/PEI/Nafion/LDHNS/DNA without (e) and with (f) 1.0×10^{-3} mol·L^{-1} phenformin hydrochloride.

Figure 7A shows the electrochemical responses of phenformin hydrochloride at bare GCE, GCE/PEI/Nafion/LDHNS and GCE/PEI/Nafion/LDHNS/DNA biosensor. No electrochemical responses were observed at both bare GCE and GCE/PEI/Nafion/LDHNS. For GCE/PEI/Nafion/LDHNS/DNA biosensor, both the oxidation peak current of the guanine and adenine decreased significantly after adding 1.0 mmol·L^{-1} phenformin hydrochloride (curve e and f in Fig 7A), owing to the specific interaction between the phenformin hydrochloride and DNA chain. Figure 7B shows the corresponding DPV curves of the biosensor, which displays more evident peak current decrease after adding the phenformin hydrochloride, indicating that the biosensor is highly responsive to the phenformin hydrochloride. We further explored the Nyquist plots of the biosensor response to the phenformin hydrochloride in 10 mmol·L^{-1} $K_3[Fe(CN)_6]$/ $K_4[Fe(CN)_6]$ aqueous solution. As shown in Figure 7C, the R_p value increased dramatically after adding 1.0 mmol·L^{-1} phenformin hydrochloride. We speculate that the adsorption of the phenformin hydrochloride on DNA chains hinders the diffusion of the $[Fe(CN)_6]^{3-/4-}$ probe to the electrode surface through the pores of the film, thus leading to an increase of the electric resistance [31]. Furthermore, the adsorption of the phenformin hydrochloride also blocks the electron transfer between DNA chain and the electrode, which results in the decrease of the oxidation peak current of the guanine [32]. As a consequence, the GCE/PEI/Nafion/LDHNS/DNA biosensor is proper for the detection of phenformin hydrochloride through recording the decrease of the electrochemical signal of the DNA.

3.4.2 Detection of phenformin hydrochloride

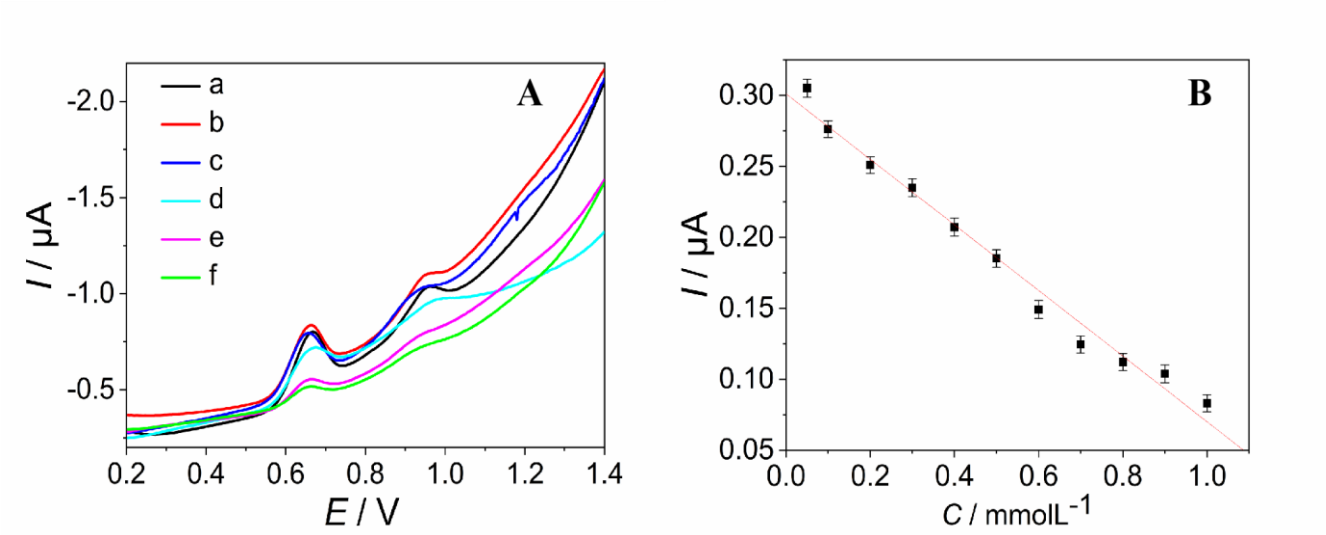

Figure 8. (A)DPVs of GCE/PEI/Nafion/LDHNS/DNA in PBS (pH 7.0) with different concentrations of phenformin hydrochloride (a) 0, (b) 1×10^{-6} mol·L^{-1}, (c) 1×10^{-5} mol·L^{-1}, (d) 1×10^{-4} mol·L^{-1}, (e) 5×10^{-4} mol·L^{-1}, (f) 1×10^{-3} mol·L^{-1}. (B)Plots of DPV peak current of GCE/PEI/Nafion/LDHNS/DNA vs concentrations of phenformin hydrochloride in PBS (pH 7.0).

To evaluate the dectection performance of the GCE/PEI/Nafion/LDHNS/DNA biosensor for phenformin hydrochloride quantitatively, we employed the DPV measurements and recorded variation

of the oxidation peak currents with the phenformin hydrochloride concentration. As is shown in the Figure 8A, both peak currents decreased with the increase of the phenformin hydrochloride concentration, suggesting the excellent electroanalytical performance of the biosensor. We recorded the peak current of the guanine oxidation as the indicator signal. As shown in Figure 8B, the peak current of guanine was found to have a linear relationship with the concentration of phenformin hydrochloride in the range of 1.0×10^{-5} mol·L^{-1} to 1.0×10^{-3} mol·L^{-1}. The detection limit is determined to be 3.4×10^{-6} mol·L^{-1} at signal-to-noise of 3. A comparison of the electroanalytical performance of our electrochemical biosensor with other reported methods for the detection of phenformin hydrochloride is listed in Table 1. The linear range of the electrochemical biosensor is dramatically larger than those of other detection methods, demonstrating the excellent electroanalytical performance of our DNA-based electrochemical biosensor for the detection of phenformin hydrochloride.

Table 1. Comparison of several methods for the detection of phenformin hydrochloride

Method	Linear range (μM L^{-1})	LOD (μM L^{-1})	Reference
TLC-DSERS	–	41.0	[33]
HPLC	21.0 - 62.0	0.27	[34]
Capillary electrophoresis	6.0 - 90.0	–	[35]
MI-FIC	0.38 - 8.3	0.021	[22]
Electrochemical biosensor	10.0 -1000.0	3.4	This work

3.5 Study of the interaction between DNA and phenformin hydrochloride

DNA is considered a promising drug target which provides an effective way for drug designing and drug screening. Studying the interaction between the drug molecules and DNA target is helpful to understand the pathogenesis of some diseases, but also has an important significance in elucidating the structure and function of DNA. In general, the interaction between DNA and drug molecules involves three binding modes [36]: (i) electrostatic binding, (ii) groove binding and (iii) intercalative binding. Many efforts have been developed to study the drug-DNA interactions, such as electrochemistry [37], UV spectroscopy [38] and fluorescence [39]. However, the interaction of DNA and phenformin hydrochloride has not been revealed yet, especially in DNA electrochemical biosensor. In the following section, we explored the interaction between DNA and phenformin hydrochloride in our biosensor through electrochemical and UV-vis spectroscopy method.

3.5.1 Electrochemical Method

We employed the double-stranded DNA (dsDNA) and single-stranded DNA (ssDNA) for fabricate the biosensor to explore the interaction between DNA chain and phenformin hydrochloride.

Figure 10 shows the DPV response of the dsDNA- and ssDNA-based biosensors after adding 6.0×10^{-4} mol·L^{-1} phenformin hydrochloride. For ssDNA-based biosensor, the oxidation peak current of guanine decreased by about 16.30%, while a 60.92% decrease was observed for the dsDNA-based biosensor. This indicates that the interaction between dsDNA and phenformin hydrochloride is stronger compared with those of ssDNA.

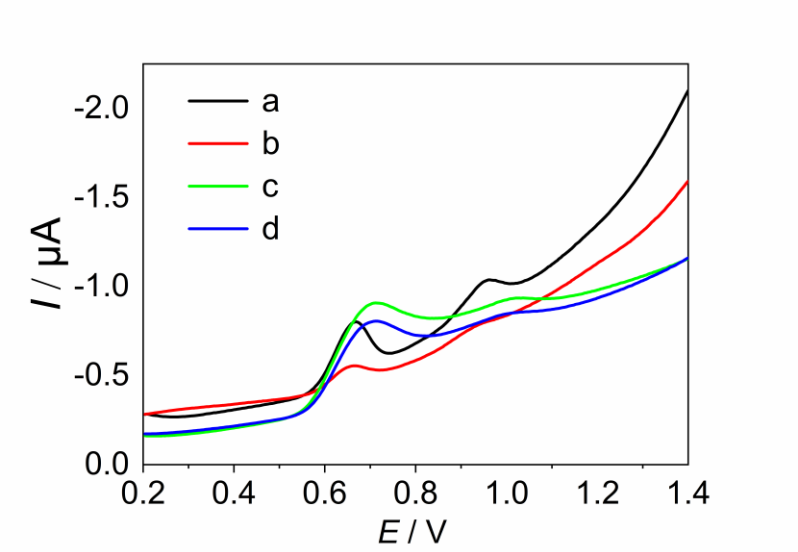

Figure 10. DPVs of GCE/PEI/Nafion/LDHNS/dsDNA (a,b) and GCE/PEI/Nafion/LDHNS/ssDNA (c,d) before (a,c) and after (b,d) adding 6.0×10^{-4} mol·L^{-1} phenformin hydrochloride in PBS (pH 7.0).

The decrease of the peak current of ssDNA-based biosensor is possibly attributed to the electrostatic interaction. Considering that the double helix structure of the dsDNA chain, the phenformin hydrochloride can also embed into the double helix to form the complex, leading to a combination interaction of the electrostatic binding and intercalative binding, which further shields the electron transfer [40]. Through analyzing the decrease ratio for the peak current, the intercalative binding is speculated to be the dominant one.

3.5.2 UV-vis spectroscopy Method

To verify the interaction between DNA and phenformin hydrochloride, we performed the UV-vis spectroscopy measurement, which is generally employed to study the binding of DNA with small molecules [41]. Figure 11A shows the UV-vis spectra of the phenformin hydrochloride and DNA. The phenformin hydrochloride exhibits an absorption peak about at 230 nm, which is in agreement with the previous report [17]. With the increase of the DNA concentration, the hypochromicity occurs that the absorption of phenformin hydrochloride decreases (Figure 11B), indicating that the interaction between phenylformin hydrochloride and DNA is dominated by intercalative binding [42]. The intrinsic binding constant can be depicted by the following equation [43]:

$$\frac{[DNA]}{(\varepsilon_\alpha - \varepsilon_f)} = \frac{[DNA]}{(\varepsilon_b - \varepsilon_f)} + \frac{1}{k_b(\varepsilon_b - \varepsilon_f)}$$

where [DNA] is the DNA concentration, ε_α, ε_f and ε_b are the apparent extinction coefficient for the free compound and fully DNA-bound combination, K_b is the binding constant, which can be obtained from the plots of [DNA]/(ε_α-ε_f) versus [DNA].

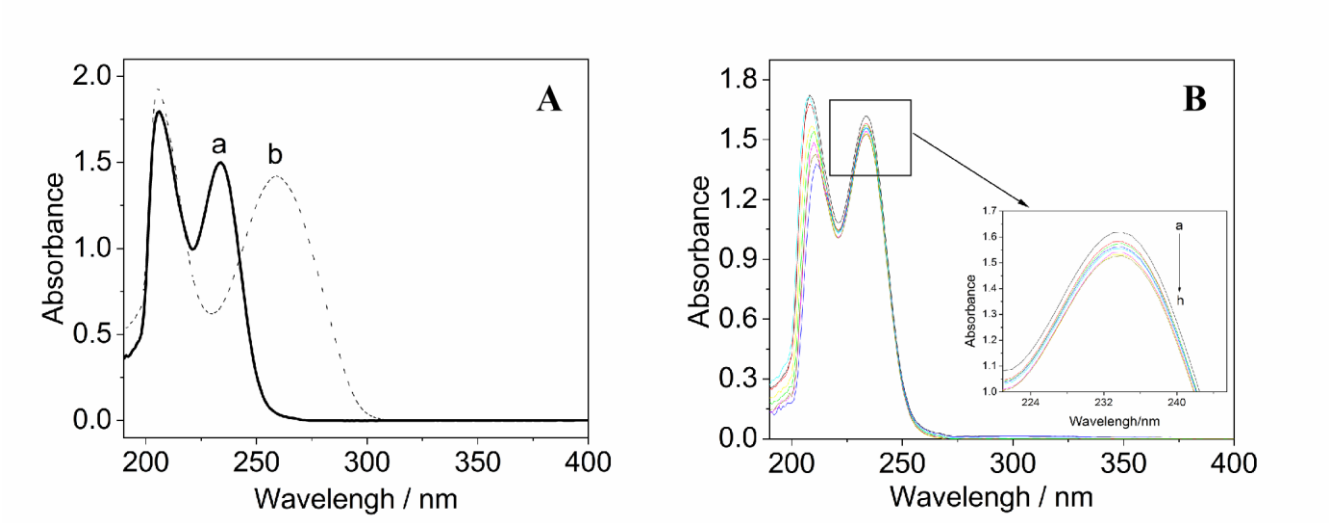

Figure 11. (A) UV-vis absorption spectra of 1×10^{-4} mol·L^{-1} phenformin hydrochlorid (a) and 2×10^{-5}mol·L^{-1} DNA (b). (B) UV-vis absorption spectra of 1.0×10^{-4} mol·L^{-1} phenformin hydrochloride with different concentrations of dsDNA in pH 7.0 PBS, (a) 0; (b) 3.0×10^{-5} mol·L^{-1}; (c) 6.0×10^{-5} mol·L^{-1}; (d) 9.0×10^{-5} mol·L^{-1}; (e) 1.2×10^{-4} mol·L^{-1}; (f) 1.5×10^{-4} mol·L^{-1}; (g) 1.8×10^{-4} mol·L^{-1}; (h) 2.1×10^{-4} mol·L^{-1}.

The K_b of phenformin hydrochloride was calculated to be 2.04×10^4 L·mol^{-1}. This value is similar to those of DNA intercalator drugs in previous reports, such as quercetin of 3.1×10^4 L·mol^{-1} [44] , sumatriptan of $5.6\pm0.2\times10^4$ L·mol^{-1} [45] and valacyclovir of 3.3×10^4 L·mol^{-1} [46]. It further proves that the interaction between the phenformin hydrochloride and DNA is mainly intercalative binding, which is in agreement with the result from the electrochemical method.

3.6 Stability and repeatability study

Stability experiment was carried out by recording the changes of the peak current of GCE/PEI/Nafion/LDHNS/DNA biosensor after placing in the refrigerator from 1 h to 24 h. The peak current decreased by about 10% after 6 h, and 15% after 24h, indicating the biosensor shows an excellent stability. Repeatability experiment was carried out by comparing the changes of peak current of five individual biosensors under the same testing conditions. The peak current varies slightly with the relative standard deviation of 0.67%, which suggests that the biosensor possesses a good repeatability.

4. CONCLUSIONS

In this paper, a novel DNA electrochemical sensor based on layered double hydroxide nanosheets film through layer-by-layer self-assembly technique was developed. This sensor has three unique advantages. Firstly, the layered double hydroxide nanosheets with good biocompatibility were employed to provide a favorable micro-environment for DNA to improve the electroanalysis performance. Secondly, we used a unique modification method, layer-by-layer self-assembly technique, which offers an easy process and allows to control the multilayer formation in a molecular scale. Finally, this DNA electrochemical sensor used the electrochemical signals of DNA bases itself, which avoids adding any other electroactive indicators and simplifies the experimental process. The sensor was successfully applied to detect phenformin hydrochloride. We believe this method will offers a new way for fabricating high-performance DNA electrochemical sensors.

ACKNOWLEDGMENTS
Financial support from the Henan Educational Committee (Grant No. 20B350007) is gratefully acknowledged.

References

1. M. X. Lu, Y. J. Deng, Y. Luo, J. P. Lv, T. B. Li, J. Xu, S. W. Chen, J.Y. Wang, *Analytical Chemistry*, 91(2019)888.
2. F. Sun, Z. C. Wang, *Materials Letters*, 234(2019)62.
3. Y. Wang, C. Yin, Q. F. Zhuang, *Journal of Alloys and Compounds*, 827(2020)154335.
4. T. G. Drummond, M. G. Hill, J. K. Barton, *Nature Biotechnology*, 21(2003)1192.
5. X. Chen, X. E. Zhang, Y. Q. Chai, W. P. Hu, Z. P. Zhang, X. M. Zhang, E. G. Anthony, *Biosensors and Bioelectronics*, 13(1998)451.
6. J. C. Andle, J. T. Weaver, J. F. Vetelino, D. J. Mcallister, *Sensors and Actuators B-chemical*, 24(1995)129.
7. L. K. Shpigun, E. Y. Andryukhina, *Journal of Analytical Methods in Chemistry*, 2019(2019)1.
8. C. Li, X. L. Hu, J. Y. Lu, X. X. Mao,Y. Xiang, Y. Q. Shu, G. X. Li, *Chemical Science*, 9(2018)979.
9. S. K. Chan, Y. S. Choong, D. Pererab, T. S. Lim, *Analytical Methods*, 10(2018)214.
10. M. Zhang, H. Hai, F. Y. Zhou, J. C. Zhong, J. P. Li, *Chinese Journal of Analytical Chemistry*, 46(2018)203.
11. T. Kulikova, A. Porfireva, G. Evtugyn, T. Hianik, *Sensors*, 19(2019)469.
12. D. Tonelli, E. Scavetta, M. Giorgetti, *Analytical and Bioanalytical Chemistry*, 405(2013)603.
13. L. Desigaux, M. B. Belkacem, P. Richard, J. Cellier, P. Léone, L. Cario, F. Leroux, C. Taviot-Guého, B. Pitard, *Nano Letters*, 6(2006)199.
14. L. M. Liu, L. P. Jiang, F. Liu, G. Y. Lu, E. S. Abdel-Halimb, J. J. Zhu, *Analytical Methods*, 5(2013)3565.
15. W. Y. Shi, Y. K. Jia, S. M. Xu, Z. X. Li, Y. Fu, M. Wei, S. X. Shi, *Langmuir*, 30(2014)12916.
16. L. X. Zhang, P. Li, X. F. Bu, J. W. Wu, X. L. Zhang, B. Zhao, Y. Tian, *Analytical and Bioanalytical Chemistry*, 410(2018)7599.
17. X. R. Zhang, J. G. Jiang, Z. H. Du, *Chinese Journal of Pharmaceuticals*, 26(1995)20.
18. B. X. Wang, H. Y. Zhu, J. Ding, *Chinese Journal of Pharmaceuticals Analyst*, 28(2008)368.
19. F. Fang, J. Yin, B. J. Shi, *Strait Pharmaceutical Journal*, 23(2011)73.
20. Z. G. Zhang, J. Wang, *The Journal of Pharmaceutical Practice*, 16(1998)358.

21. B. Y. Deng, A. H. Shi, Y. H. Kang, *Luminescence*, 26(2011)592.
22. Z. B. Liu, F. Y. Jia, W. W. Wang, C. X. Wang, Y. M. Liu, *Luminescence*, 26(2012)297.
23. S. Sangribsub, P. Tangboriboonrat, T. Pith, G. Decher, *Polym Bull*, 53(2005)425.
24. J. B. Han, J. Lu, M. Wei, Z. L. Wang, X. Duan, *Chemical Communications*, 41(2008)5188.
25. R. Z. Ma, Z. P. Liu, L. Li, N. Iyi, T. Sasaki, *Journal of Materials Chemistry*, 16(2006) 3809.
26. F. B. Kaufman, A. H. Schroeder, E. M. Engler, S. R. Krame, J. Q. Chambers, *Journal of the American Chemical Society*, 102(1980)483.
27. C. Tersch, F. Lisdat, *Electrochimica Acta*, 56(2011)7673.
28. D. W. Pang, M. Zhang, Z. L. Wang, Y. P. Qi, J. K. Cheng, Z. Y. Liu, *Journal of Electroanalytical Chemistry*, 403(1996)183.
29. P. Alvarez, M. J. Castanon, A. J. M. Ordieres, P. T. Blanco, *Electroanalysis*, 16(2004)1193.
30. Z. P. Zhao, Y. L. Qi, M. Wei, F. Z. Zhang, S. L. Xu, *Materials Letters*, 78(2012)62.
31. C. Amatore, J. M. Saveant, D. Tessier, *Journal of Electroanalytical Chemistry*, 147(1983)39.
32. X. Q. Lu, Y. Chen, J. Chen, Y. Zhang, L. M. Zhang, M. R. Li, *International Journal of Electrochemical Scienc*e, 1(2006)130.
33. F. Fang, Y. P. Qi, F. Lu, L. B. Yang, *Talanta*, 146(2016)351.
34. J. H. Lin, Y. T. Lin, Y. J. Huang, K. C. Wen, R. M. Chen, T. H. Ueng, C. H. Liao, *Journal of Food and Drug Analysis*, 9(2001)6.
35. E. P. C. Lai, S. Y. Feng, *Journal of Chromatography B-Analytical Technologies in the Biomedical and Life Sciences*, 843(2006)94.
36. R. Y. Zhang, D. W. Pang, R. X. Cai, *Chemical Journal of Chinese Universities*, 20(1999)1210.
37. S. Rauf, J. J. Gooding, K. Akhtar, M. A. Ghauri, M. Rahman, M. A. Anwar, A. M. Khalid, *Journal of Pharmaceutical and Biomedical Analysis*, 37(2005)205.
38. H. W. Gao, W. Q. Xu, *Analytica Chimica Acta*, 458(2002)417.
39. W. Y. Zhong, J. S. Yu, Y. Q. Liang, *Spectrochimica Acta Part A: Molecular and Biomolecular Spectroscopy*, 59(2003)1281.
40. H. X. Ju, Y. K. Ye, Y. L. Zhu, *Electrochimica Acta*, 50(2005)1361.
41. J. P. Cheng, Q. Y. Lin, R. D. Hu, W. Z. Zhu, H. Q. Li, D. H. Wang, *Journal of Chemical Physics*, 7(2009)105.
42. J. F. Peng, J. Y. Ling, H. X. Zhang, C. K. Zhang, *Spectroscopy and Spectral Analysis*, 24(2004)858.
43. M. Purcell, J. F. Neault, T. Riahi, *Biochimica et Biophysica Acta*, 1487(2000)61.
44. S. Bi, C. Qiao, D. Song, Y. Tian, D. Gao, Y. Sun, H. Zhang, *Sensors and Actuators B: Chemical*, 119(2006)199.
45. N. Shahabadi, N. H. Moghadam, *Spectrochimica Acta Part A: Molecular and Biomolecular Spectroscopy*, 99(2012)19.
46. N. Shahabadi, N. Fatahi, M. Mahdavi, Z. K. Nejad, M. Pourfoulad, *Spectrochimica Acta Part A: Molecular and Biomolecular Spectroscopy*, 83(2011)20.